Hydrothermal and Dry-heat Treatments in Merocyanine-containing Langmuir-Blodgett Films

Hiroko Moshino, Yuki Koyano, Yuichi Sugano, Yasuhiro F. Miura and Michio Sugi

Graduate School of Engineering, Toin University of Yokohama, 1614 Kurogane-cho, Aoba-ku, Yokohama 225-8502, Japan

Fax: 81-45-972-5972, e-mail: sugi@cc.toin.ac.jp

Hydrothermal and dry-heat treatments (HTT and DHT, respectively) are studied on the mixed LB films of a merocyanine and Cd arachidate. The HTT process under 100%-humidity condition is found to involve two stages: the as-deposited J-band first dissociates and then a new phase of J-band appears to grow associated with round-shaped superstructure as large as up to ~0.1 mm in diameter. The DHT process under dry ambient dissociates the original J-band without appreciable changes in film texture. The first stage of HTT terminates within 1 min at temperatures higher than 60°C, while the J-band peak after DHT at 60°C for 30 min retains ca. 85% of its original height. X-ray diffraction reveals that the LB lamellar structure remains intact in both HTT and DHT processes with an enhanced ordering of Cd ion alignment. As for the role of the water content, the lubrication effect is preferred to the hydration effect.

Key words: Langmuir-Blodgett films, Merocyanine chromophores, Formation of superstructures, Hydrothermal treatments, Dry-thermal treatments

1. INTRODUCTION

A merocyanine dye MS shown in Fig. 1 (a) is a well-known film-forming molecule for constructing functional Langmuir-Blodgett (LB) films [1-8]. MS forms stable monolayers on a Cd^{2+}-containing water subphase with pH range of 6.2 to 6.4 when they are diluted with arachidic acid (C_{20} in Fig. 1 (b)). Both MS and C_{20} form salts with Cd^{2+}, and thus prepared MS-C_{20} mixed monolayers are readily deposited to form Y-type LB films. Under a usual subphase condition, pH=6.5 at 20°C, e.g., the films are bluish in color and associated with a redshifted J-band with its absorption maximum located at ~590 nm. Here, the J-band is known to originate from a specific type of dipole-coupled array that is often referred to as a J-aggregate [9]. For smaller pH-values, pH=5.5, e.g., however, the J-band is no more predominant, and the films are now reddish in color [10].

As is well known, the aggregation state of MS in the LB films can be systematically modified by various secondary treatments. There are many reports on the dissociation-restoration processes of the J-aggregates [6, 11-19]. The J-aggregate is dissociated and restored by acid and basic treatments (AT and BT, respectively, in both liquid and vapor phases [6, 11]. As for the heat treatments (HT), two different consequences have been found in the spectral changes. One is the dissociation of the J-band induced by a heat-treatment under dry ambient (dry-heat treatment, DHT), which turns the film color from bluish to reddish [6, 11]. The other is the J-band reorganization induced by a hydrothermal treatment (HTT) under 100% relative humidity, forming a new phase of J-aggregate with the spectra further redshifted and sharper in shape than those before the treatment [14-18]. Here, it is noted that the water content remaining on the sample has been found to be responsible for the two different consequences of the "mild" HTs, i.e., HTT-type and DHT-type, are essentially identical with those induced by HTT and DHT, respectively [12, 13, 19].

Recently, we have shown that HTT induces not only the reorganization of the original J-band but also drastic changes in the film texture [16-19]. After HTT, the
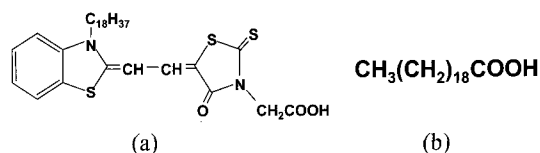

$$CH_3(CH_2)_{18}COOH$$

(a)   (b)

Fig. 1 Chemical formulas of the film-forming materials: (a) merocyanine (MS), and (b) arachidic acid (C_{20}).

photomicroscopic image, initially anisotropic and featureless, is found to tend to isotropic and filled with round-shaped superstructures as large as up to ~0.1 mm in diameter [16, 18]. After DHT, however, no superstructures are seen, while the initial anisotropy tends to decrease as the process proceeds [6, 19]. The present paper aims to characterize the HTT and the DHT processes based on the results of optical measurements, photomicroscopic observations and X-ray diffraction measurements for the better understanding of the color-phase transitions in the MS-C_{20} mixed LB system.

2. EXPERIMENTAL

MS and C_{20} were purchased from Hayashibara Biochemical Lab. Inc. and Fluka AG, respectively, and used without further purification. They were dissolved in optical-grade chloroform from Tokyo Kasei with a molar mixing ratio of [MS] : [C_{20}]=1 : 2. The substrates, each 1/4 of an ordinary slide glass (13 mm×38 mm and 1 mm thick). After cleaned as described previously [6], they were then hydrophobized by either coating with five monolayers of C_{20} or exposing them to 1, 1, 1, 3, 3, 3-hexamethyldisilazane (HMDS) vapor. Ten MS-C_{20} monolayers were deposited onto one side of each substrate using the vertical dipping technique as described previously [6, 14-16]. The films were of Y-type with a deposition ratio of approximately unity. The samples were stored in a silica gel desiccator to remove the remaining water content. An aluminum tube (ca. 20 mm in diameter and 150 mm long) with a screw top at one end was employed for both HTT and DHT with and without introducing a small amount of pure water (2 cm^3 or less) into the tube, respectively [14-15]. After the LB
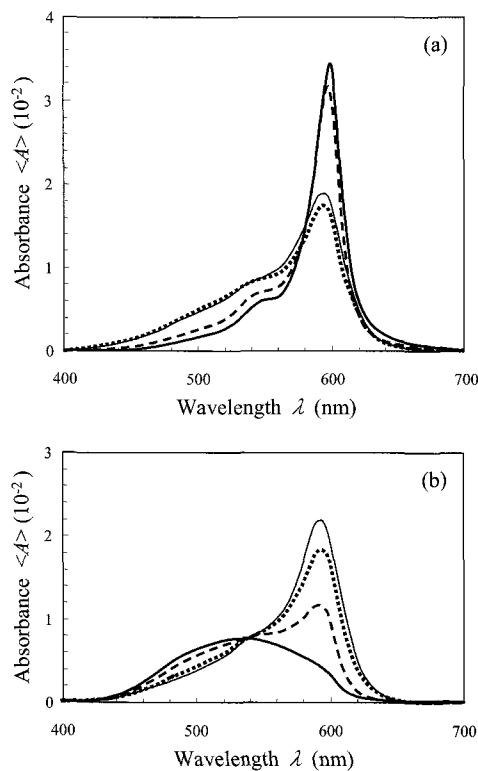
Fig. 2 Absorbance spectra per monolayer $<A>$ of MS-C_{20} mixed LB films. (a) The dotted, dashed and solid lines refer to the cases after HTT for t_H=60 min at T_H=30, 60 and 90°C, respectively. (b) The dotted, dashed and solid lines refer to the cases after DHT for t_H=30 min at T_H=60, 75 and 90°C, respectively. The as-deposited case is shown by the thin solid lines in both (a) and (b).

Fig. 3 Difference spectra per monolayer $\Delta(<A>)$= $<A(t_H)> - <A(0)>$. The solid and dotted lines refer to HTT at T_H=65°C for t_H=1 min and DHT at T_H=90°C for t_H=5 min, respectively.

sample was enclosed, the tube was immersed in a water bath as described previously [14-16]. UV-visible absorption spectra $A_\parallel$ and $A_\perp$ were measured using a Shimadzu UV-2100 spectrometer, where $A_\parallel$ and $A_\perp$ refers to linearly polarized light incidents with the electric vector parallel and perpendicular to the direction of dipping and raising, respectively. The film texture was observed using an Olympus BH-2 microscope with a CCD camera. The X-ray diffraction profiles were measured using a Rigaku Denki RINT2000 diffractometer (Cu Kα source, wavelength λ=1.54 Å, X-ray tube voltage and current: 50 kV and 300 mA, respectively).

3. RESULTS AND DISCUSSION
3.1 Spectral changes induced by HTT and DHT

The HTT-induced reorganization is found for heating temperatures T_H=30 – 90°C. Figure 2 (a) shows the average spectra $<A>=(A_\parallel+A_\perp)/2$ per monolayer after 30-min HTT, where $<A>$ excludes the apparent change due to the varying in-plane anisotropy. A typical $<A>$ spectrum in the as-deposited state is also shown in the figure. The dichroic ratio $R=A_\parallel/A_\perp$ at the original J-band peak usually falls in a range of 1.2 – 2.5 depending on the deposition condition, and $R \rightarrow 1$ (i.e., isotropic) as the HTT process proceeds. The HTT-induced process involves two different stages as
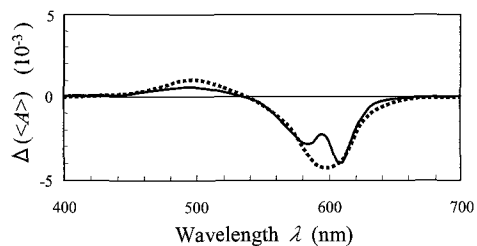
preliminarily reported [17]. In the first stage, a crossover point is recognized at ~540 nm between the spectra before and after HTT with the level of $<A>$ at the shorter wavelengths increasing and the J-band component correspondingly decreasing [14, 17]. The second stage is characterized by the growth of the reorganized J-band with an isosbestic point at ~570 nm. For the 30 min-HTT case, the $<A>$-spectrum at T_H=30°C represents the first stage, while those at T_H=60°C and 90°C belong to the second stage. Here, it is noted that the growth of the J-band peak in the second stage can be approximated by an exponential saturation function for a fixed t_H with a rate constant increasing with T_H [17].

The spectral changes induced by DHT are shown in Fig. 2 (b), where the $<A>$ spectra per monolayer after 30-min DHT are given together with a typical as-deposited $<A>$ spectrum. The J-band monotonically decreases with T_H, and almost completely disappears for T_H=90°C [6]. The crossover point in a range of 530 – 540 nm seen among the spectra may be identified with that recognized in the first stage of HTT process. The decrease in the J-band height can be presumably approximated by an exponential decay function for a fixed t_H with a rate constant increasing with T_H [17]. The J-band peak after DHT at T_H=60°C for t_H=30 min retains ~85% of its initial height.

3.2 Decrease in the J-band component in the first stage of HTT

Figure 3 shows the difference spectrum $\Delta(<A>)$= $<A(t_H)> - <A(0)>$ after HTT for t_H=1 min at T_H=65°C, where the $\Delta(<A>)$ spectrum after DHT for t_H=5 min at T_H=90°C is added for comparison. Both $\Delta(<A>)$ curves share common tendency in spite of the difference in both t_H and T_H: each curve shows a crossover point at λ~540 nm and the $\Delta(<A>)$-values are positive and negative at the shorter and the longer wavelengths, respectively. In the previous papers, we have shown that the $<A>$ spectra before and after HTT and DHT can be deconvoluted into three components, Band I, Band II and Band III (whose peak located around λ=500 – 515 nm, 545 – 555 nm and 590 – 600nm, respectively, and that Band I, Band II and Band III are presumably assigned as dimers, monomers and J-aggregates [14, 17]. Therefore, the positive and negative $<A>$-values at the left and right of the crossover point indicates that Band I increases at the expense of Band III with Band II tending to remain unchanged for both HTT and DHT. For the HTT case, we recognize a small maximum at ~595 nm associated with a pair of valleys. The second stage
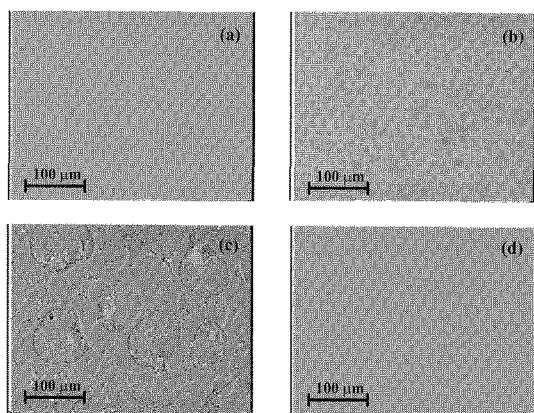
Fig. 4 Photomicrographs of ten-layered MS-C$_{20}$ mixed LB films: (a) As-deposited state, (b) after HTT at 70°C for 1 min, (c) after HTT at 70°C for 60 min, and (d) after DHT at 90°C for 60 min.

Fig. 5 X-ray diffraction profiles of ten-layered MS-C$_{20}$ mixed LB films deposited on HMDS-hydrophobized substrates measured using a Cu-Kα source. (a), (b) and (c) refer to the patterns in the as-deposited state, after HTT at T_H=70°C for t_H=60 min, and after DHT at T_H=90°C for t_H=60 min, respectively.

growth of the reorganized J-band has therefore begun to proceed for t_H=1 min at T_H=65°C.

Two curves resemble to each other in both shape and order of magnitude except for the above-mentioned small maximum for the HTT case. The dissociation rate $\Delta(<A>)/\Delta t_H$ ~4×10^{-3} min^{-1} for 65°C-HTT in the first stage is therefore estimated to be about five times larger than ~8×10^{-4} min^{-1} for 90°C-DHT (see, Fig. 3).

3.3 Changes in texture induced by the heat treatments

Figure 4 exemplifies the images for different cases. As shown in Fig. 4 (a), the image for the as-deposited state is featureless with an associated vague local inhomogeneity within the resolution of the microscope, although the present MS-C$_{20}$ as-deposited films are known to be phase-separated into MS-rich and C$_{20}$-rich domains of submicrometer size. The anisotropy observed for the spectra in the as-deposited state is reflected as the brightness of the image varying with a π-periodicity when the sample is rotated on the stage in accordance with $R = A_\parallel/A_\perp > 1$. The image after HTT for t_H=1 min at T_H=70°C is shown in Fig. 4 (b). Round-shaped domains are seen, each 10 – 20 μm in diameter with a bright rim. The anisotropy is found to remain observable in this stage as the π-periodicity of the brightness. Figure 4 (c) refers to the case of HTT with t_H=60 min at T_H=70°C. Another type of domains, the dark-rimmed, are now clearly seen besides the bright-rimmed domains whose size is increased up to a 30 – 60 μm in diameter, and the π-periodicity in brightness is no more recognized. Figure 4 (d) refers to the case of DHT at T_H=90°C for 60 min. The image after DHT closely resembles to that in the as-deposited state (see, Fig. 4 (a)), featureless with an associated vague local inhomogeneity, except for the π-periodicity which decreases as the process proceeds in accordance with the spectral change.

3.4 X-ray diffraction measurements

The X-ray diffraction profiles are shown in Fig. 5 for the as-deposited, HTT at T_H=70°C for t_H=60 min and DHT at T_H=90°C for t_H=30 min, each using an HMDS-treated substrate to eliminate the possible signals from the C$_{20}$ monolayers, where the diffraction angle is
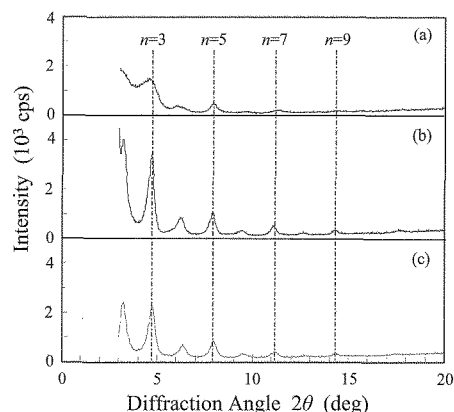
limited to $3° < 2\theta < 20°$. The as-deposited state is referred to in Fig. 5 (a). As is well known, the diffraction peaks correspond to the Cd–Cd spacing between the adjacent Cd ion lattice planes aligned at the hydrophilic interfaces, i.e., the thickness of the Y-type bilayer unit cell (~2×27.6 Å for C$_{20}$-based Y-type LB films) [11, 16]. The centrosymmetry of the cell is reflected in each even-numbered diffraction peak that is lower in height than the neighboring odd-numbered ones. The peaks are relatively broad in width and low in intensity, and we clearly recognize those for n=3 – 9 except for n=8, where n denotes the order of diffraction. These results coincide well with those previously reported for the MS-C$_{20}$ mixed LB films [11, 16]. After HTT, the diffraction angle of each peak remains almost unchanged as shown in Fig. 5 (b). The peaks are recognizable up to n=11, and the intensity of each peak remarkably increases associated with a narrowing in width as previously reported [16]. The peak intensity for n=5, e.g., is increased by a factor of 2 or more after HTT. It is indicated that HTT has an annealing effect to enhance the ordering of Cd ion lattice alignment. A similar increase in peak intensity with narrowing is found after DHT as shown in Fig. 5 (c), indicating the enhanced ordering of Cd ion alignment. In the DHT case, however, the J-band is not reorganized but simply dissociated in contrast.

3.5 Possible role of the water content in the HTT process

The significant difference between the HTT and DHT processes indicates the crucial role of the water content supplied from the ambient of 100% humidity in the HTT-induced reorganization process of the J-band accompanied by the formation of the round-shaped superstructures. Two different effects are so far considered, i.e., the lubrication and the hydration [14-19]. The lubrication effect may lower the energy barriers of microbrownian motions that are more or less hindered in the LB system, while the hydration effect may dissociate the ionic bonds which stabilize the film structure.

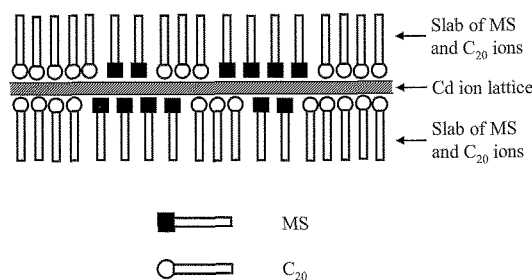The unit cell of the present LB system can be

Fig.6 Schematic representation of the bilayer unit cell of an MS-C_{20} LB film.

compared to a Cd^{2+} ion lattice sandwiched between a pair of negatively charged slabs, each consisting of $[C_{20}]^-$ and $[MS]^-$ anions with their CH_3- and $-COO^-$ groups at the outer and the inner sides, respectively, as schematically shown in Fig. 6 [16]. The unit cell is stabilized by the ionic bonds formed between the positively charged Cd^{2+} ion lattice and the negatively charged slab pair, and also by the van der Waals forces that gather together the constituents. In the lubrication effect, the H_2O molecules can appreciably reduce the van der Waals forces by their larger polarizabilities resulting in the reorganization of MS chromophores and the long hydrocarbon groups without significantly affecting the ionic bonds. The cell structure will be however drastically changed by H^+ and OH^- ions introduced into the system, leading to degradation of the Cd^{2+} ion lattices, if the hydration effect predominates in the HTT process.

The results of X-ray diffraction measurement present a crucial reference for preferring the lubrication effect to the hydration effect. The ordering of the Cd^{2+} ion lattices is found to be enhanced in both HTT and DHT cases as we have seen in Sect. 3.4. The remarks on the dissociation rates $\Delta(<A>)$ for both cases (Sect. 3.2) also indicate the lubrication effect to soften the aggregation state resulting in the enhanced mobility.

4. CONCLUDING REMARKS

We have described two different types of heat treatments applied to the MS-C_{20} mixed LB films, HTT under condition of 100% humidity and DHT in the dry ambient. The results are summarized in the following items.

1) HTT involves two stages, the dissociation of the as-deposited J-band followed by the growth of the reorganized J-band, while the DHT process is characterized as a monotonic decay of the J-band.

2) HTT is typically observed in a wide temperature range of T_H=30 – 90°C, while the typical DHT processes are confined to the higher temperature range.

3) HTT is accompanied by the formation and growth of the round-shaped superstructures, while no significant change in texture is observed for the DHT.

4) Both HTT and DHT enhance the ordering of the Cd^{2+} ion lattice, and the Cd-Cd spacings for both cases are identifiable with each other.

5) The lubrication effect is preferred to the hydration effect as to the role of the water content to soften the film resulting in the enhanced mobility of the molecules

The HTT and DHT processes are complementary to each other in the sense that the former reorganizes and

the latter dissociates the J-band. Both HTT and DHT are gas-phase processes which are carried out with lower risk of contamination in comparison to the liquid-phase processes. It is suggested that HTT, and DHT as well, serves as an effective means to modify the physical properties of LB films without degradation of their original lamellar structure.

It is noted that he HTT process is a unique case of the simultaneous occurrence of in-plane superstructures and the enhanced ordering of the LB lamellar structure. Although the present study is focused on the changes in the optical absorbance and the texture, preliminary experiments are under way in view of other physical properties. The results will be published elsewhere.

REFERENCES

[1] M. Sugi and S. Iizima: *Thin Solid Films* **68**, 199 (1980).
[2] M. Sugi, M. Saito, T. Fukui and S. Iizima: *Thin Solid Films* **99**, 17 (1983).
[3] S. Kuroda, M. Sugi and S. Iizima: *Thin Solid Films* **99**, 21 (1983).
[4] M. Saito, M. Sugi, T. Fukui and S. Iizima: *Thin Solid Films* **100**, 117 (1983).
[5] K. Sakai, M. Saito, M. Sugi and S. Iizima: *Jpn. J. Appl. Phys.* **24**, 365 (1985).
[6] M. Sugi, M. Saito, T. Fukui and S. Iizima: *Thin Solid Films* **129**, 15 (1985).
[7] H. Nakahara, K. Fukuda, D. Mobius and H. Kuhn: *J. Phys. Chem.* **90**, 6144 (1986).
[8] S. Nishikawa, Y. Tokura, T. Koda and K. Iriyama: *Jpn. J. Appl. Phys.* **25**, L701 (1986).
[9] See, for example, "J-aggregates", Ed. by T. Kobayashi, World Scientific, Singapore (1996).
[10] M. Sugi: unpublished data.
[11] M. Saito, M. Sugi, K. Ikegami, M. Yoneyama and S. Iizima: *Jpn. J. Appl. Phys.* **25**, L478 (1986).
[12] J. Miyata, S. Morita, Y. F. Miura and M. Sugi: *Jpn. J. Appl. Phys.* **44**, 8110 (2005).
[13] J. Miyata, S. Morita, Y. F. Miura and M. Sugi: *Colloids Surf.* A **284-285**, 509 (2006).
[14] S. Mouri, J. Miyata, S. Morita, Y. F. Miura and M. Sugi: *Trans. Mater. Res. Soc. Jpn.* **31**, 573 (2006).
[15] S. Mouri, S. Morita, Y. F. Miura and M. Sugi: *Jpn. J. Appl. Phys.* **45**, 7925 (2006).
[16] S. Mouri, H. Moshino, S. Hasegawa, Y. F. Miura and M. Sugi: *Jpn. J. Appl. Phys.* **46**, 1650 (2007).
[17] H. Moshino, S. Hasegawa, S. Mouri, Y. F. Miura and M. Sugi: *Trans. Mater. Res. Soc. Jpn.* **32**, 305 (2007).
[18] S. Hasegawa, H. Moshino, S. Mouri, Y. F. Miura and M. Sugi: *Trans. Mater. Res. Soc. Jpn.* **32**, 309 (2007).
[19] M. Sugi, H. Moshino, S. Hasegawa, S. Mouri and Y. F. Miura: *Trans. Mater. Res. Soc. Jpn.* **32**, 313 (2007).